



Jaypee University of Information Technology
Solan (H.P.)
LEARNING RESOURCE CENTER

Acc. Num. ~~SP04108~~ Call Num:
SP04108

General Guidelines:

- ◆ Library books should be used with great care.
- ◆ Tearing, folding, cutting of library books or making any marks on them is not permitted and shall lead to disciplinary action.
- ◆ Any defect noticed at the time of borrowing books must be brought to the library staff immediately. Otherwise the borrower may be required to replace the book by a new copy.
- ◆ The loss of LRC book(s) must be immediately brought to the notice of the Librarian in writing.

Learning Resource Centre-JUIT



SP04108

FULL WAVE ANALYSIS OF RECTANGULAR MICROSTRIP PATCH ANTENNA AT MILLIMETER WAVE FOR COMMUNICATION SYSTEMS

By

ABHISHEK SHARMA – (041023)

SANDEEP.MATCHA-(041035)

ABHISHEK KUMAR SINHA – (041102)



MAY-2008

**Submitted in partial fulfillment of the Degree of Bachelor of
Technology**

Project Guide: Dr. Ghanshyam Singh

**DEPARTMENT OF ELECTRONICS AND
COMMUNICATION**

**JAYPEE UNIVERSITY OF INFORMATION TECHNOLOGY
WAKNAGHAT.**

CERTIFICATE

This is to certify that the work entitled, "Full Wave analysis of rectangular patch antenna at millimeter wave for communication" submitted by Abhishek Sharma, Abhishek Kumar Sinha and Matcha Sandeep for the award of degree of Bachelor of Technology in Electronics & Communication of Jaypee University of Information Technology has been carried out under my supervision. This work has not been submitted partially or wholly to any other University or Institute for the award of this or any other degree or diploma.



Dr. G.SINGH

Project Guide

Department of Electronics & Communication.

ACKNOWLEDGMENT

Though this project batch consists of only three members, it would be very wrong on our part to call this project a result of the efforts of just three individuals. In fact, we would like to call this a collective effort, as we had received assistance from various quarters during the development of our project. We take this opportunity to thank each and everyone who have helped us.

First and foremost, we thank our Guide, Mr. Ghanshyam Singh, who in spite of his various engagements, always found time for us, and without whose assistance, the entire project would never have borne fruits. Actually, words will not reflect on the amount of help that we have got from our Guide.

We also would like to thank Dr Harinder Singh (HOD-Mathematics department) , who assisted us time to time during the progress of our work.

We thank the Department of Electronics & communication, JUIT, for providing us the necessary facilities to work on our project.

Abhishek Sharma
(ABHISHEK SHARMA) (041023)

M. Sandeep
(MATCHA SANDEEP) (041035)

(ABHISHEK KUMAR SINHA) (041102)

Table of contents	PAGE
List of figures.....	1
Abstract.....	3
Methodology.....	4
CHAPTER 1 INTRODUCTION.....	5
1.1 INTRODUCTION OF ANTENNA	5
1.1.1 WORKING OF ANTENNA.....	5
1.2 MICROSTRIP ANTENNA.....	5
1.2.1 ADVANTAGE OF MICROSTRIP ANTENNA.....	6
1.2.2 LIMITATIONS OF MICROSTRIP ANTENNA.....	6
1.3 FEEDING TECHNIQUES OF MICROSTRIP ANTENNA.....	7
1.4 COXAIL FEED/PROBE FEED.....	7
1.4.1 ADVANTAGES OF PROBE FEED.....	8
1.4.2 LIMITATIONS OF PROBE FEED.....	8
1.5 MICROSTRIP FEED.....	8
1.5.1 LIMITATIONS OF MICROSTRIP FEED.....	9
1.6 APERTURE-COUPLED MICROSTRIP FEED.....	9
1.7 COMPARISON OF VARIOUS TYPE OF FEEDING TECHNIQUES.....	11
CHAPTER 2 MODEL OF ANALYSIS.....	12
2.1 THE TRANSMISSION LINE MODEL.....	12
CHAPTER 3 MODEL OF ANALYSIS.....	15
3.1 THE CAVITY MODEL.....	15
CHAPTER 4 FULL WAVE MODEL OF ANALYSIS.....	20
4.1 FEATURES OF FULL WAVE ANALYSIS.....	20
4.2 SPECTRAL DOMAIN FULL WAVE ANALYSIS.....	20

4.2 SPECTRAL DOMAIN FULL WAVE ANALYSIS.....	20
4.3 GREEN'S FUNCTION.....	20
4.4 THE SPECTRAL DOMAIN FULL WAVE APPROACH.....	20
4.5 DERIVATION OF GREEN'S FUNCTION.....	23
4.6 MOMENT OF METHOD SOLUTION.....	26
CHAPTER 5 FULLWAVE ANALYSIS USING FDTD METHOD.....	28
CHAPTER 6 RESULTS OBTAINED AFTER WORKING ON COMPUTER SIMULATION TECHNIQUE.....	32
CHAPTER 7 CONCLUSION.....	39
REFERENCES.....	40

LIST OF FIGURES

Figure	Page No.
Figure1.1 Microstrip antenna configuration	5
Figure1.2 Charge distribution and current density on a microstrip antenna	6
Figure1.3 Microstrip antenna with a coaxial Probe.....	7
Figure1.4 Canonical Problem of a parallel plate waveguide fed by a coaxial probe.....	7
Figure1.5 Equivalent circuit of a microstrip antenna fed by a probe.....	8
Figure1.6 Coplanar microstrip feeding.....	9
Figure1.7 Equivalent circuit diagram of microstrip feeding	9
Figure1.8 Aperture couple feeding.....	10
Figure1.9 Aperture couple microstrip feed.....	10
Figure2.1 Microstrip line.....	12
Figure2.2 Effective dielectric constant.....	12
Figure3.1 Cavity model.....	15
Figure3.2 Rectangular microstrip patch geometry.....	15
Figure3.3 Field configurations for various modes.....	16
Figure3.4 Current distributions on four sides of patch.....	17
Figure3.5 Field and magnetic current densities for radiating slots.....	17
Figure3.6 Predicted and measured E- AND H-plane pattern	18
Figure3.7 Current density n non radiating slots of rectangular microstrip antenna.....	19
Figure4.1 Geometry of a rectangular microstrip antenna with a probe feed	21
Figure4.2 Geometry of a horizontal electric dipole.....	24
Figure6.1 S- parameter polar plot.....	32
Figure6.2 Voltage standing wave ratio with frequency.....	33
Figure6.3 Far field 'far field (directivity) radiation pattern at frequency $f=9.018$	33
Figure6.4 Far field 'far field (directivity) radiation pattern at frequency $f=16.523$	33
Figure6.5 Far field 'far field (Axial Ratio) radiation pattern at frequency $f=16.523$	34
Figure6.6 Far field 'far field ($f=16.523$)[1] Directivity abs[Theta].....	34
Figure6.7 Far field 'far field ($f=9.018$)[1] Directivity Right Polarization[theta].....	34
Figure6.8 Far field 'far field ($f=9.018$)[1] Axial ratio[theta].....	35

Figure6.9 Far field 'far field (f=16.523)[1]'H-field [r=1m]_Right Polarization [Theta].....	35
Figure6.10 Far field 'far field (f=16.523) [1]'H-field [r=1m] _ Left Polarization [Theta]...	35
Figure6.11 Far field 'far field (f=9.018) [1]'H-field [r=1m] _ Left Polarization [Theta].....	36
Figure6.12 Far field 'far field (f=16.523) [1]' Axial ratio [Theta].....	36
Figure6.13 Far field 'far field (f=16.523) [1]'Right Polarization [r=1m]_Phi [Theta].....	36
Figure6.14 Far field 'far field (f=9.018)[1]'Right Polarization [r=1m]_Phi [Theta].....	37
Figure6.15 Far field 'far field (f=9.018)[1]'Left Polarization [r=1m]_Phi [Theta].....	37
Figure6.16 Far field 'far field (f=16.523) [1]'E-field [r=1m] _Theta [Theta]	37
Figure6.17 Far field 'far field (f=9.018)[1]'Gain Theta [Theta].....	38
Figure6.18 Far field 'far field (f=16.523) [1]'Directivity Left Polarization [Theta].....	38

ABSTRACT

An antenna is an essential component of wireless communication systems that is needed in both the transmitting and receiving terminals. In this project, an analysis of special type of antenna called microstrip patch antenna is presented. Microstrip patch antennas are used in several wireless applications such as global positioning system (GPS) receivers and radar systems. In this project we have tried to analyze rectangular patch antenna by using three methodologies namely (1) Transmission line model (2) Cavity model (3) Full wave analysis. Primarily we have focused on full wave analysis. We have used METHOD OF MOMENTS and GREEN'S FUNCTION to arrive at our analytical solution.

For the simulation part we have used CST MICROWAVE STUDIO Software to attain desired results. The frequency range selected is from 1-20 GHz. The CST Software uses the Finite difference time domain (FDTD) technique in which analytical processing and modeling are almost absent unlike other numerical techniques.

METHODOLOGY

The main objective of this work is to use three types of techniques namely:

- 1) Transmission line model
- 2) Cavity model
- 3) Full wave analysis.

We have tried to focus on full wave analysis by adopting GREEN'S FUNCTION and METHOD OF MOMENTS.

We have used technique in the spectral domain to develop a full wave analysis of rectangular patch microstrip antenna. The spectral domain full wave approach uses the exact green's function for the mixed dielectric nature of the antenna. The green's function is employed in the electric field integral equation formulation to satisfy the boundary conditions at the patch metallization. The resulting integral equations are discretized into a set of linear equations by means of moment method to yield a matrix equation. The solution of matrix equation provides the current distribution on the patch metallization. The near and far field characteristics of the antenna are then obtained from current distribution and Green's function.

For the simulation part we have used CST MICROWAVE STUDIO Software to attain desired results. The frequency range selected is from 1-20 GHZ. The CST Software uses the Finite difference time domain(FDTD) technique in which analytical processing and modeling are almost absent unlike other numerical techniques.

CHAPTER 1

1.1 INTRODUCTION

An antenna is a transducer between a guided wave and a free space wave or vice-versa. The data to be transmitted from point a to point through the atmosphere has to be converted from its electrical form inside the transmitter into an electromagnetic wave that can propagate through the atmosphere to reach the receiver station where it is converted back to an electrical signal for further processing the part that converts electrical signals into electromagnetic wave and vice versa is called antenna.

1.2 MICROSTRIP ANTENNA

Microstrip antenna consists of a radiating patch on one side of a dielectric substrate ($\epsilon_r \geq 1$) which has a ground plane on the other side [1].

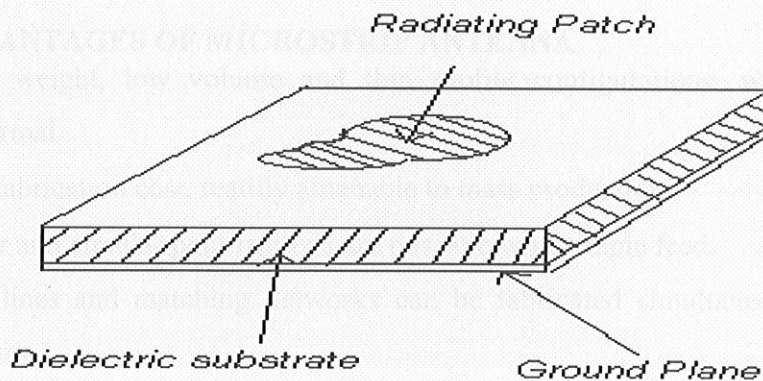


Fig 1.1 Microstrip patch antenna configuration.

Whenever a microstrip antenna is excited by a feed, there will be charge distribution on the upper and lower surfaces of patch as well as on the surface of ground plane [2]. The occurrence of charges is due to supply by a microwave source. We take it as a sine wave, so when there is supply from positive half cycle on the patch there will be positive charge distribution on the patch, as a result there will be negative charge distribution on the ground plane. When negative cycle of the sine wave will be supplied there will be negative charge on the ground plane, as a result there will be positive charge on ground. So there will be force

of attraction between opposite charges but there will also be force of repulsion between same charges which are on the patches well as on the ground plane.

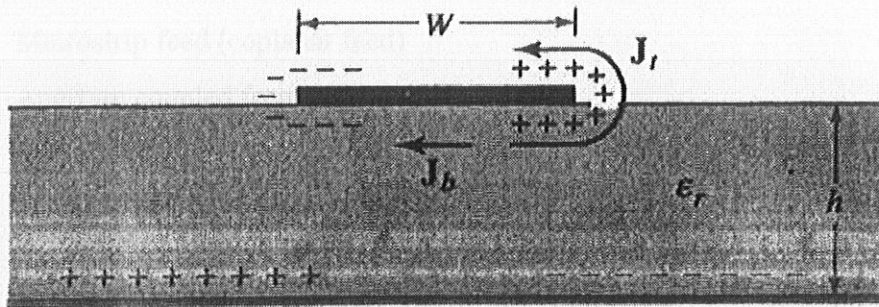


Fig 1.2 The charge distribution and current density on a microstrip patch antenna.

So net electric field will be cancelled out and there will be fringing effect due to charges which are present at the edges and this fringing effect will cause radiation [3].

1.2.1 ADVANTAGES OF MICROSTRIP ANTENNA

- Light weight, low volume and thin profile configurations, which can be made conformal.
- Low fabrication cost, readily amenable to mass production.
- Linear and circular polarizations are possible with simple feed.
- Feed lines and matching networks can be fabricated simultaneously with antenna structure.
- Can be easily integrated with microwave integrated circuits.

1.2.2 LIMITATIONS OF MICROSTRIP ANTENNA

- Narrow bandwidth and associated tolerance problems.
- Large ohmic loss in feed structure of arrays.
- Complex feed structures required for high performance arrays.
- Excitation of surface wave.
- The antennas are sensitive to environmental factors like temperature and humidity.

1.3 FEEDING TECHNIQUES OF MICROSTRIP ANTENNA

There are three main feeding techniques:

- Coaxial Feed/Probe feed
- Microstrip feed (coplanar feed)
- Aperture coupled feed

1.4 COAXIAL FEED/PROBE FEED

This feed comes from the ground plane by having through hole in the substrate [5]. The coaxial connector is attached to the backside of the circuit board, and the coaxial centre conductor after passing through the substrate is soldered to the patch metallization [15]. The location of feed point is determined so that best impedance match is achieved.

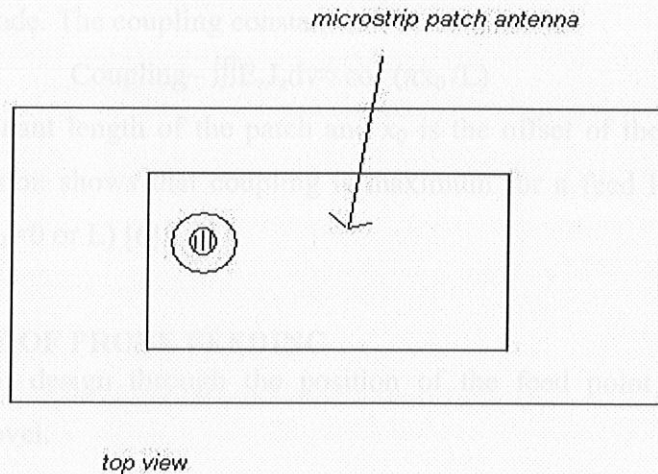


Fig 1.3 Microstrip patch antenna with a coaxial probe.

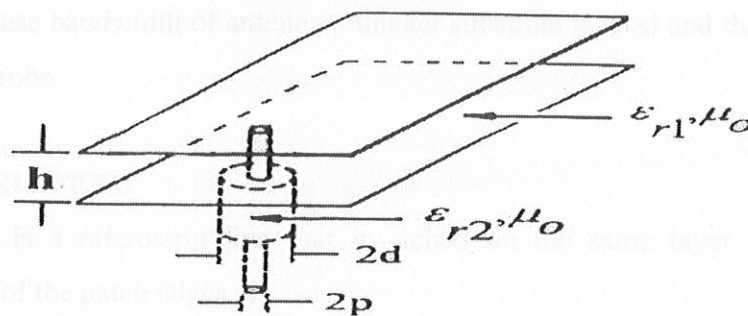


Fig 1.4 Canonical problem of a parallel late waveguide fed by the coaxial probe.

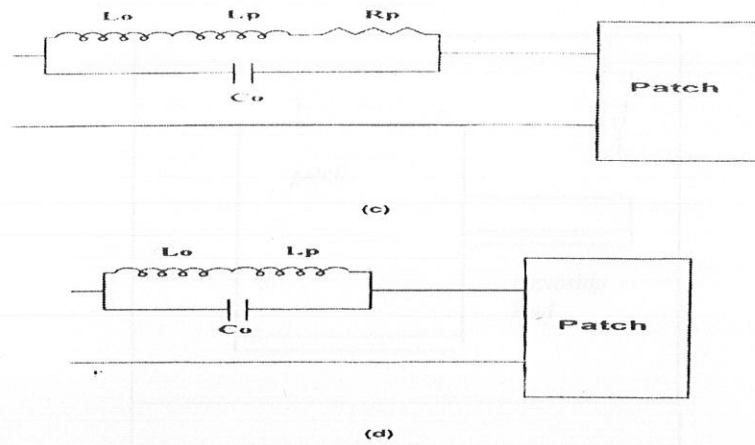


Fig 1.5 Equivalent circuit of a microstrip patch antenna fed by a probe.

Excitation of the patch occurs principally through the coupling of the feed current J_z to the E_z field of the patch mode. The coupling constant can be obtained as:

$$\text{Coupling} \sim \iiint E_z J_z dv \approx \cos(\pi x_0/L)$$

where L is the resonant length of the patch and x_0 is the offset of the feed point from the patch edge. Expression shows that coupling is maximum for a feed located at a radiating edge of the patch ($x_0=0$ or L) [6].

1.4.1 ADVANTAGE OF PROBE FEEDING

- Simplicity of design through the position of the feed point to adjust the input impedance level.

1.4.2 LIMITATIONS OF PROBE FEEDING

- It requires a large number of solder joints which makes fabrication difficult.
- To increase bandwidth of antenna a thicker substrate is used and therefore requires a longer probe.

1.5 MICROSTRIP FEED

This feed line is a microstrip line that is etched on the same layer as the patch and connects to one of the patch edges [7].

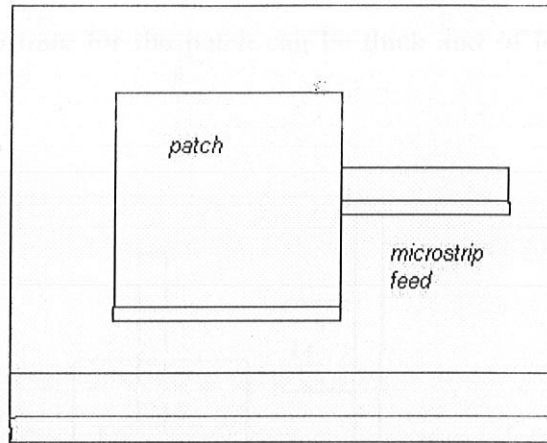


Fig 1.6 Coplanar microstrip feeding.

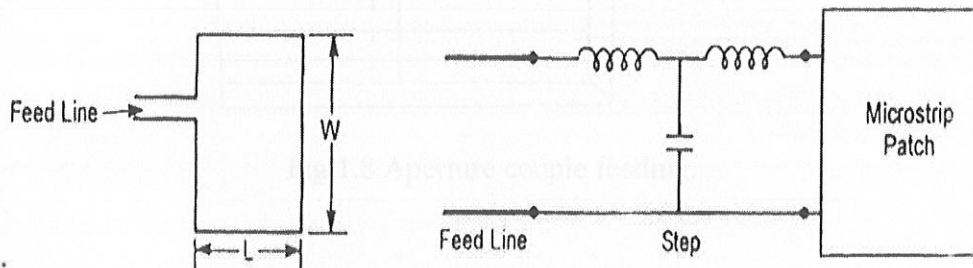


Fig 1.7 Equivalent circuit diagram.

1.5.1 LIMITATIONS OF MICROSTRIP FEED

- There is impedance mismatch because the input impedance of the patch at its radiating edge is very high compared to the impedance of feed line [16].
- The microstrip line blocks the radiation from the portion of which it is in contact resulting in reduced radiation.

1.6 APERTURE-COUPLED MICROSTRIP FEED

This type of feeding technique uses two substrate separated by a common ground plane [8]. A microstrip feed line on the lower substrate is electromagnetically coupled to the patch through a slot aperture in the common ground plane [9]. The substrate parameters for the two layers are chosen in a manner to optimize the field and radiation functions independently [10]. For example the substrate for the feed line should be thin and of high dielectric

constant, whereas the substrate for the patch can be thick and of lower dielectric constant [13].

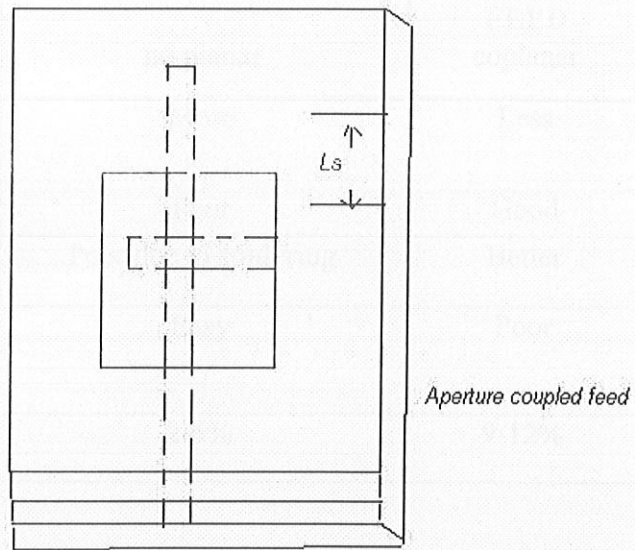


Fig 1.8 Aperture couple feeding.

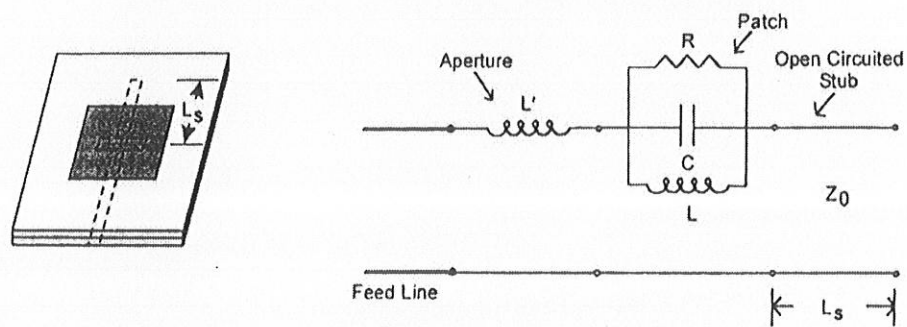


Fig 1.9 Aperture coupled microstrip feed.

1.7 COMPARISON OF VARIOUS TYPE OF FEEDING TECHNIQUES

characteristics	COAXIAL PROBE FEED	MICROSTRIP FEED	APERTURE COUPLED
Configuration	no planar	coplanar	planar
Spurious feed radiation	More	Less	More
Ease of fabrication	Poor	Good	Excellent
Reliability	Poor due to soldering	Better	Good
Impedance matching	Easy	Poor	Easy
bandwidth	2-5%	9-12%	21%



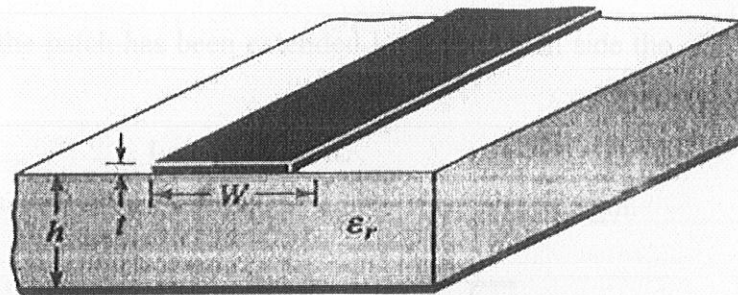
(c) Effective dielectric constant

Fig 2.2, Effective Dielectric Constant

- It is a non-homogeneous line of two dielectrics, typically substrate and air. Most of the electric field lines in the substrate and parts of some lines exist in air an effective dielectric constant is introduced to account for fringing and the wave propagation in the line. For a line with air above substrate effective dielectric constant has value in the range.
- The effective dielectric constant is a function of frequency. As the frequency of operation increases, most of the electric field lines concentrate in the substrate, so lines behave more like a homogeneous line of one dielectric [22].
- Dimension of the patch has been extended along the length from each end by a distance $0l$, which is a function of effective dielectric constant ϵ_{eff} and the width to height ratio is W/H .

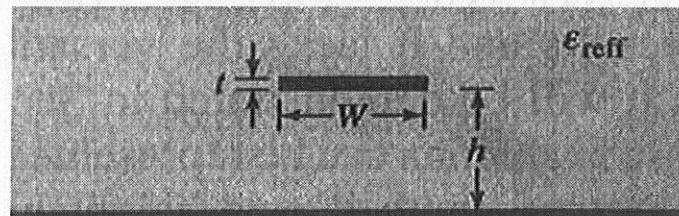
CHAPTER 2

TRANSMISSION LINE MODEL



(a) Microstrip line

Fig 2.1 Microstrip Line



(c) Effective dielectric constant

Fig 2.2. Effective Dielectric Constant

- It is a non-homogeneous line of two dielectrics, typically substrate and air. Most of the electric field lines in the substrate and parts of some lines exist in air an effective dielectric constant is introduced to account for fringing and the wave propagation in the line. For a line with air above substrate effective dielectric constant has value in the range.
- The effective dielectric constant is a function of frequency. As the frequency of operation increases, most of the electric field lines concentrate in the substrate. So lines behave more like a homogeneous line of one dielectric [22].
- Dimension of the patch has been extended along the length from each end by a distance δl , which is a function of effective dielectric constant ϵ and the width to height ratio is W/H .

$$\frac{\Delta L}{h} = 0.402 \frac{(\epsilon_{\text{reff}} + 0.3) \left(\frac{W}{H} + 0.264 \right)}{(\epsilon_{\text{reff}} - 0.258) \left(\frac{W}{H} + 0.8 \right)}$$

Since the length of the patch has been extended by ΔL on each side the effective length of patch is now:

$$L_{\text{eff}} = L + 2 \Delta L$$

For Resonant frequency of a microstrip antenna is a function of length.

$$(f_r)_{010} = \frac{v_0}{2L\sqrt{\epsilon_r}}$$

It does not account for fringing effect. It must be modified to include edge effects and it should be computed as:

$$\begin{aligned} (f_{rc})_{010} &= \frac{1}{2L_{\text{eff}} \sqrt{\epsilon_{\text{reff}}} \sqrt{\mu_0 \epsilon_0}} = \frac{1}{2(L + 2\Delta L) \sqrt{\epsilon_{\text{reff}}} \sqrt{\mu_0 \epsilon_0}} \\ &= q \frac{1}{2L \sqrt{\epsilon_r} \sqrt{\mu_0 \epsilon_0}} = q \frac{v_0}{2L \sqrt{\epsilon_r}} \end{aligned}$$

$$q = \frac{(f_{rc})_{010}}{(f_r)_{010}}$$

- The q factor is referred to as fringing factor. As the substrate height increases fringing also increases.
- Design procedure is as follows

Specify:

$$\epsilon_r, f_r \text{ (hz)}, h$$

Determine:

W, L

- For an efficient radiator, a practical width that leads to good radiation efficiencies is:

$$W = \frac{1}{2f_r \sqrt{\mu_0 \epsilon_0}} \sqrt{\frac{2}{\epsilon_r + 1}} = \frac{v_0}{2f_r} \sqrt{\frac{2}{\epsilon_r + 1}}$$

“Where V is free space velocity of wave”

The input resistance for inset feed is given by:

$$R_{in}(y=y_0) = \frac{1}{(G_1 + G_{12})} \left[\cos^2\left(\frac{\Pi}{L} y_0\right) + \frac{G_1^2 + B_1^2}{Y_c^2} \sin^2\left(\frac{\Pi}{L} Y_0\right) - \frac{B_1}{Y_c} \sin\left(\frac{2\Pi}{L} Y_0\right) \right]$$

$$R_{in}(Y = Y_0) = \frac{1}{2(G_1 \pm G_2)} \cos^2\left(\frac{\Pi}{L} Y_0\right)$$

Maximum value occurs at the edge of slot ($Y_0 = 0$) where voltage is maximum and current is minimum, minimum value of (zero) occurs at the centre of the patch, where the voltage is zero and current is maximum.

Fig. 3.1 Cavity model

The vector potential must satisfy the following equation [27]

The solution is given by separation of variables method as follows.

$$A_z = [A_1 \cos(k_x x) + B_1 \sin(k_x x)] [A_2 \cos(k_y y) + B_2 \sin(k_y y)] [A_3 \cos(k_z z) + B_3 \sin(k_z z)]$$

Applying the following boundary conditions for the patch geometry shown below:

$$E_z(x=0, 0 \leq y \leq L, 0 \leq z \leq W) = 0$$

$$E_z(x=h, 0 \leq y \leq L, 0 \leq z \leq W) = 0$$

$$H_z(0 \leq x \leq h, 0 \leq y \leq L, z=0) = 0$$

$$H_z(0 \leq x \leq h, 0 \leq y \leq L, z=W) = 0$$

$$H_z(0 \leq x \leq h, y=0, 0 \leq z \leq W) = 0$$



Fig. 3.2 Rectangular microstrip patch antenna geometry.

Solving for boundary conditions we get the electric and magnetic field given by

CHAPTER 3

CAVITY MODEL

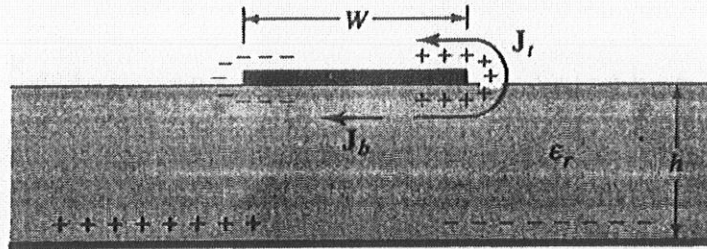


Fig 3.1 Cavity model

- The vector potential must satisfy the following equation [27].
- The solution is given by separation of variable method as follows.

$$A_x = [A_1 \cos(k_x x) + B_1 \sin(k_x x)] [A_2 \cos(k_y y) + B_2 \sin(k_y y)] [A_3 \cos(k_z z) + B_3 \sin(k_z z)]$$

Applying the following boundary conditions for the patch geometry shown below:

$$E_y (x' = 0, 0 \leq y' \leq L, 0 \leq z' \leq w) = 0$$

$$= E_y (x' = h, 0 \leq y' \leq L, 0 \leq z' \leq W) = 0$$

$$H_y (0 \leq x' \leq h, 0 \leq y' \leq L, z' = 0) = 0$$

$$= H_y (0 \leq x' \leq h, 0 \leq y' \leq L, z' = W) = 0$$

$$H_z (0 \leq x' \leq h, y' = 0, 0 \leq z' \leq W) = 0$$

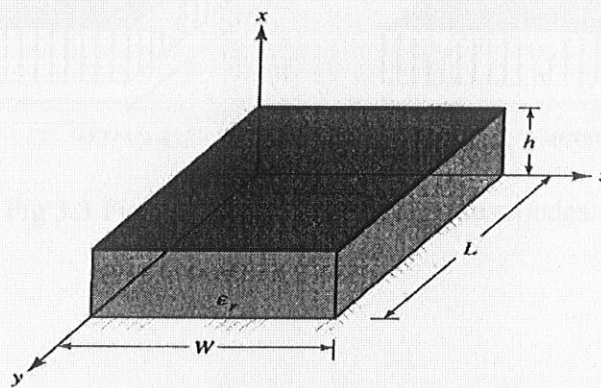


Fig 3.2 Rectangular microstrip patch antenna geometry.

- Solving for boundary conditions we get the electric and magnetic field given by:

$$E_x = -j \frac{(k^2 - k_x^2)}{\omega \epsilon \mu} A_{mnp} \cos(k_x x') \cos(k_y y') \cos(k_z z')$$

$$E_y = -j \frac{k_x k_y}{\omega \epsilon \mu} A_{mnp} \sin(k_x x') \sin(k_y y') \sin(k_z z')$$

$$E_z = -j \frac{k_x k_z}{\epsilon \mu \omega} A_{mnp} \sin(k_x x') \sin(k_y y') \sin(k_z z')$$

$$H_x = 0$$

$$H_y = -\frac{k_z}{\mu} A_{mnp} \cos(k_x x') \cos(k_y y') \sin(k_z z')$$

- The various resonant frequencies for different modes (dominant mode) is given by:

$$(f_r)_{010} = \frac{1}{2L \sqrt{\mu\epsilon}} = \frac{V_0}{2L \sqrt{\epsilon_r}}$$

$$(f_r)_{001} = \frac{1}{2W \sqrt{\mu\epsilon}} = \frac{v_0}{2W \sqrt{\epsilon_r}}$$

$$(f_r)_{020} = \frac{1}{L \sqrt{\mu\epsilon}} = \frac{v_0}{L \sqrt{\epsilon_r}}$$

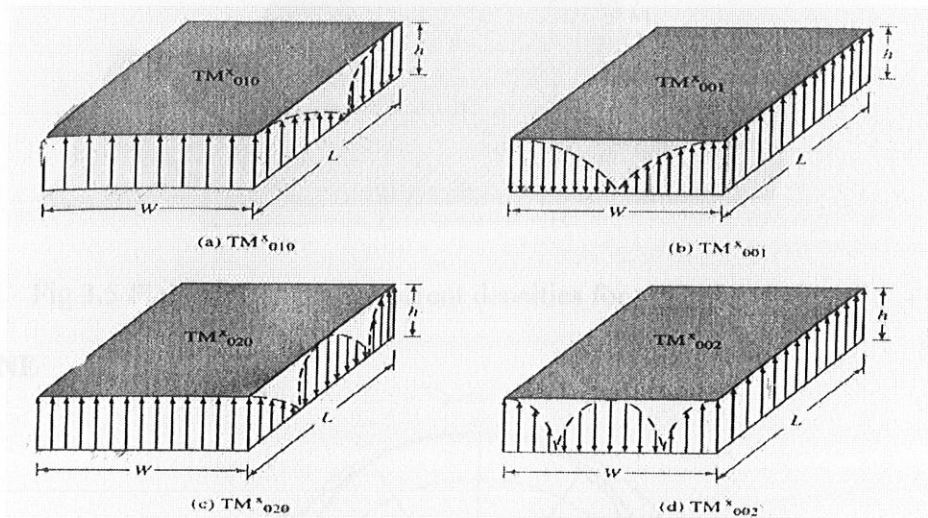


Fig 3.3 Field configurations for various modes.

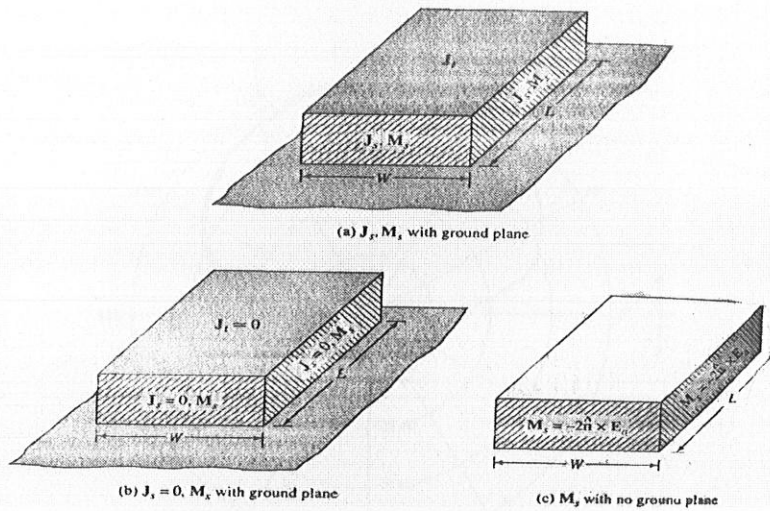


Fig 3.4 Current densities on four sides of the patch.

$$M_z = -2 \hat{n} \times E_a$$

$$j_z = \hat{n} \times H_a$$

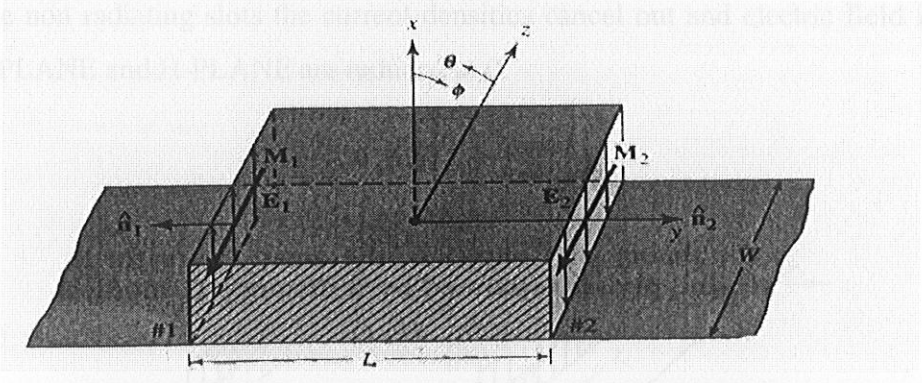
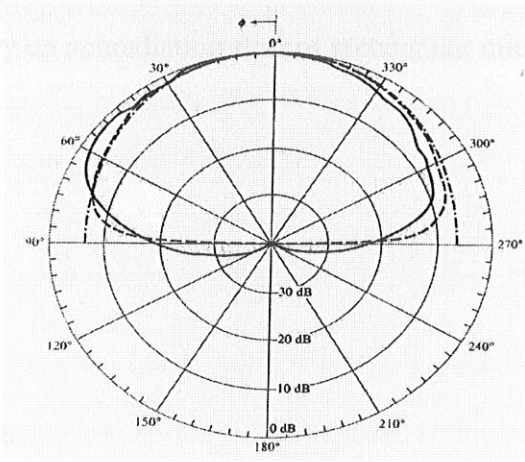


Fig 3.5 Field and magnetic current densities for radiating slots.

For E- PLANE



For H-PLANE

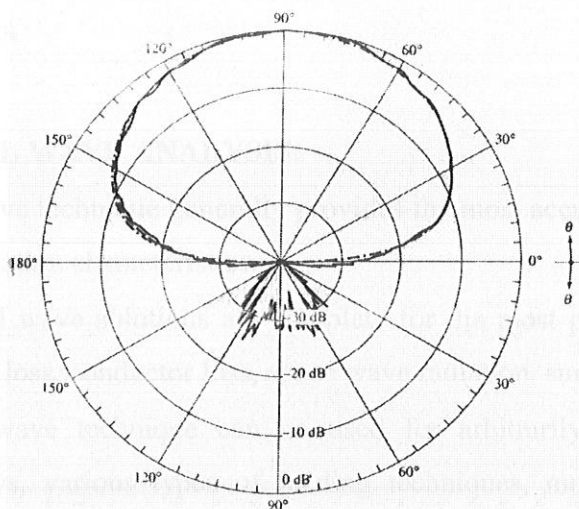


Fig 3.6 Predicted and measured E- AND H-plane patterns of rectangular microstrip patch($l=0.906\text{cm}$, $w=1.186\text{cm}$, $h=0.1588\text{cm}$, $y_0=0.3126$, $\epsilon_r=2.2$, $f_0=10\text{GHz}$)

- For the non radiating slots the current densities cancel out and electric field in both the E-PLANE and H-PLANE are reduced to 0.

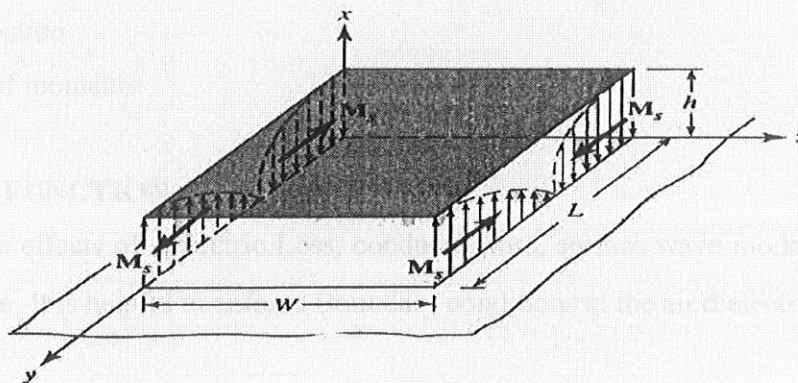


Fig 3.7 Current density on nonradiating slots of rectangular microstrip antenna

CHAPTER 4

FULL WAVE ANALYSIS

4.1 FEATURES OF FULL WAVE ANALYSIS:

- Accuracy: Full wave technique generally provides the most accurate solution for the impedance and radiation characteristics.
- Completeness: full wave solutions are complete for the most part i.e. they include effects of dielectric loss, conductor loss, space wave radiation, surface waves [16].
- Versatility- Full wave technique can be used for arbitrarily shaped microstrip elements and arrays, various types of feeding techniques, multilayer geometries, anisotropic substrates, and active antennas.
- .Computation cost- this technique is numerically intensive, and therefore require careful programming to reduce computational cost

4.2 SPECTRAL DOMAIN FULL WAVE ANALYSIS

Two main functions used in this technique are

1. Green function
- 2 .Method of moments

4.3 GREEN FUNCTION

It includes the effects of dielectric Loss, conductor loss, surface wave modes, and space wave radiation. It is helpful to enforce Boundary conditions at the air dielectric interface.

4.4 THE SPECTRAL DOMAIN FULL –WAVE APPROACH

Uses the exact Green's function for the mixed dielectric nature of the microstrip antenna. Green's function is employed in the electric field integral equation formulation to satisfy the boundary conditions at the patch metallization. The resulting integral equations are discretized into set of linear equations by means of the moment method to yield a matrix equation. The solution of the matrix equation provides the current distribution on the patch metallization [15].

The configuration of a rectangular microstrip antenna fed by a coaxial probe is shown in figure:

It consists of a metal patch on a grounded dielectric substrate. The microstrip antenna may employ inhomogeneous or mixed dielectric in the form of substrate below the patch metallization and free space above it. Because of the mixed dielectric nature, the green's function can be obtained in a closed form only in the spectral domain [22]. For the x-directed current j_x on the air-interface at $z=0$, the electric field components in the spectral domain are:

$$\tilde{E}_x(k_x, k_y, h) = \frac{-j}{\omega\epsilon_0} \left[\frac{k_x^2 k_1 k_2 \sin(k_1 h)}{\beta^2 T_m} + \frac{k_y^2 k_0^2 \sin(k_1 h)}{\beta^2 T_e} \right] j_x$$

$$E_y(k_x, k_y, h) = \frac{-j}{\omega\epsilon_0} \left[\frac{k_x k_y k_1 k_2 \sin(k_1 h)}{\beta^2 T_m} - \frac{k_x k_y k_0^2 \sin(k_1 h)}{\beta^2 T_e} \right] j_x$$

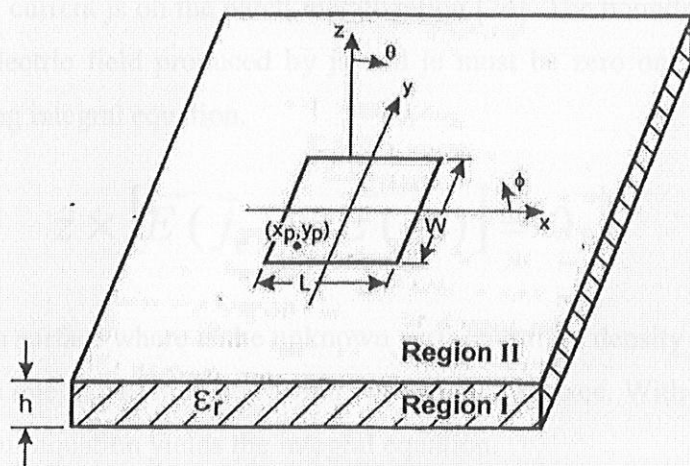


Fig 4.1 Geometry of a rectangular microstrip antenna with a probe feed .Air dielectric surface at $z=h$.

- For the y-directed current j_y on the air-dielectric interface at $z=h$, the electric field components in the spectral domain are

$$\tilde{E}_y(k_x, k_y, h) = \frac{-j}{\omega\epsilon_0} \left[\frac{k_y^2 k_1 k_2 \sin(k_1 h)}{\beta^2 T_m} + \frac{k_x^2 k_0^2 \sin(k_1 h)}{\beta^2 T_e} \right] j_y$$

Where,

$$T_m = \epsilon_r k_2 \cos(k_1 h) + j k_1 \sin(k_1 h)$$

$$T_e = k_1 \cos(k_1 h) + j k_2 \sin(k_1 h)$$

$$k_1^2 = k_z^2 = \epsilon_r k_0^2 - \beta^2, 0 < z < h, \text{Im}(k_1) < 0$$

$$\beta^2 = k_x^2 + k_y^2$$

$$\bar{E}(k_x, k_y, z) = \int_{-\infty}^{\infty} \int_{-\infty}^{\infty} E(x, y, z) e^{jk_x x} e^{-jk_y y} dx dy$$



The notation k_p clearly specifies its radial nature, but β is being retained here to help the reader with vast amount of literature using this notation for the spectral domain approach [31]. In a microstrip antenna fed by a probe current there are two types of currents j_e on the probe and the surface current j_s on the patch metallization [24]. The boundary condition that the total tangential electric field produced by j_s and j_e must be zero on the patch surface giving rise to following integral equation.

$$\hat{z} \times [\bar{E}(\bar{j}_e) + \bar{E}(\bar{j}_s)] = 0$$

For all points on patch surface where is the unknown surface current density (\bar{j}_s) is the dyadic green's function. This integration is to be carried out on patch surface. With the use of above equation in the previous equation yields the integral equation.

$$\hat{z} \times [\bar{E}(\bar{j}_e) + \int \int_s \bar{j}_s \cdot \bar{G}(x, y | x_0, y_0) dx_0 dy_0] = 0$$

For a lossy conductor the effect of ohmic losses is included by introducing a surface impedance Z_s equal to ratio of the tangential electric field to the surface current density.

$$\hat{z} \times [\bar{E}(\bar{j}_e) + \bar{E}(\bar{j}_s)] = Z_s \bar{j}_s$$

The surface impedance Z_s of a metal sheet with conductivity σ is defined as:

$$Z_s = (1 + j) \sqrt{\pi f \mu_0} / \sigma$$

The dielectric loss can be accounted for by introducing a dielectric constant $\epsilon_r(1 - j \tan \delta)$

Now to find out unknown surface current is method of moments is used. The results of method of moments can be written in matrix form

$$[Z]N \times N [I]N \times 1 [V]N \times 1, N = N_x + N_y$$

here N_x and N_y are the number x directed and y directed expansion currents

4.5 DERIVATION OF GREEN'S FUNCTION

Equivalently, a unit strength infinite small current source in the x direction is considered first.

The substrate is assumed to be lossless and ground plane is a perfect electric conductor. If the dipole source is located at (x, y) , we can express the x-directed current as:

$$j_x = \hat{x} \delta(x - x_0) \delta(y - y_0)$$

The green's function can be obtained through two different routes: the vector potential approach and direct solution of the wave equation for the $E(z)$ and $H(z)$ [31]. The latter approach involves simpler algebra and follows next.

The source free Maxwell equations with time variation $\exp(j\omega t)$ assumed and suppressed are

$$\nabla \times \bar{E} = -j\omega\mu_0 \bar{H}$$

$$\nabla \times \bar{H} = -j\omega\epsilon_0 \epsilon_r \bar{E}$$

The effect of current source $j(x)$ is included through an interface condition. The above equations are solved simultaneously to give the wave equations:

$$-\nabla \times \nabla \times \bar{E} + \omega^2 \mu_0 \epsilon_0 \epsilon_r \bar{E} = 0$$

$$-\nabla \times \nabla \times \bar{H} + \omega^2 \mu_0 \epsilon_0 \epsilon_r \bar{H} = 0$$

Applying the divergence condition $\nabla \cdot \bar{E} = 0$ to the z component and

$\nabla \cdot \bar{H} = 0$ to the z component yields the wave equations

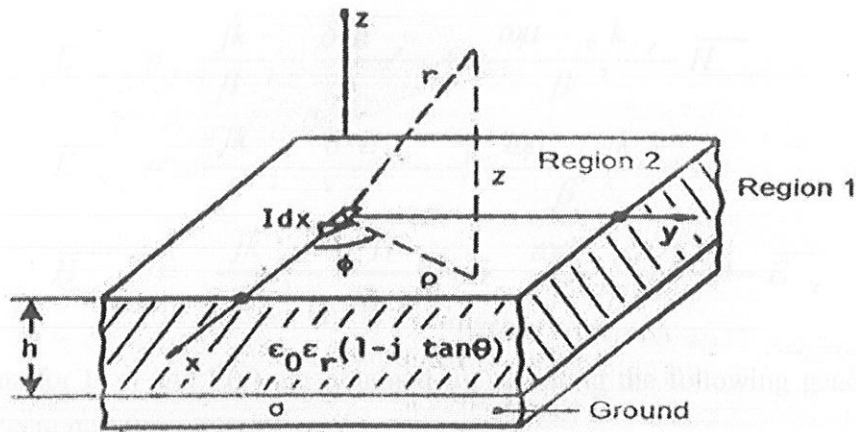


Fig 4.2 Geometry of a horizontal electric dipole on the surface of a grounded dielectric substrate.

$$\frac{\partial^2 E_z}{\partial x^2} + \frac{\partial^2 E_z}{\partial y^2} + \frac{\partial^2 E_z}{\partial z^2} + \epsilon_0 k_0^2 E_z = 0$$

$$\frac{\partial^2 H_z}{\partial x^2} + \frac{\partial^2 H_z}{\partial y^2} + \frac{\partial^2 H_z}{\partial z^2} + \epsilon_r k_0^2 H_z = 0$$

By using the most general solutions in the form of plane waves, the above equations yield

$$k_x^2 + k_y^2 + k_z^2 = k_0^2 \epsilon_r$$

Hence the propagation constant is given by

$$k_1^2 = k_z^2 = \epsilon_r k_0^2 - \beta^2, 0 \leq z \leq h$$

$$k_2^2 = k_z^2 = k_0^2 - \beta^2, z > h$$

Because the analysis is carried out in the Fourier domain, we will use Fourier transformed fields, current densities, and so on. Fourier transforms pair as follows:

$$\psi(x, y, z) = \frac{1}{4\pi^2} \iint \tilde{\psi}(k_x, k_y, z) e^{jk_x x} e^{jk_y y} dk_x dk_y$$

Maxwell's equations can be Fourier transformed to obtain the following expressions:

$$E_x = \frac{jk_x}{\beta^2} \frac{\partial \bar{E}_z}{\partial z} + \frac{\omega\mu_0 k_y}{\beta^2} \bar{H}_z$$

$$\bar{E}_y = \frac{jk_y}{\beta^2} \frac{\partial E_z}{\partial z} - \frac{\omega\mu_0 k_x}{\beta^2} H_z$$

$$\bar{H}_y = \frac{jk_y}{\beta^2} \frac{\partial H_z}{\partial z} + \frac{\omega\epsilon_0 \epsilon_r k_x}{\beta^2} \bar{E}_z$$

The solutions for E(x) and E(y) are obtained by assuming the following general forms for E(Z) and H(z) in the regions 1 and 2:

$$\bar{E}_{z2} = Ae^{-jk_2 z}$$

$$\bar{H}_{z2} = Be^{-jk_2 z}$$

$$E_{z1} = C \cos(k_1 z) + D \sin(k_1 z)$$

The constants A to F in the above equations are obtained by applying following boundary conditions:

$$\bar{E}_x = 0, z = 0$$

$$\bar{E}_y = 0, z = 0$$

Substitute for Ez and Hz in the above equations for regions 1 and 2. Now subject to the boundary conditions. After completing considerable algebraic computations one would obtain the expressions for the constants A to F resulting in the following expressions.

$$E_{z2} = \frac{k_x k_1 \sin(k_1 h)}{j\omega\epsilon_0 T_m} e^{-jk_2(z-h)j_x}$$

$$H_{z2} = \frac{-jk_y \sin(k_1 h)}{T_e} e^{-jk_2(z-h)j_x}$$

With the use of above equations in the general equations at z=h, we get.

$$\bar{E}_x(k_x, k_y, h) = \frac{-j}{\omega \epsilon_0} \left[\frac{k_x^2 k_1 k_2 \sin(k_1 h)}{\beta^2 T_m} + \frac{k_y^2 k_0^2 \sin(k_1 h)}{\beta^2 T_e} \right] j_x$$

$$\tilde{E}_y(k_x, k_y, h) = \frac{-j}{\omega \epsilon_0} \left[\frac{k_x k_y k_1 k_2 \sin(k_1 h)}{\beta^2 T_m} - \frac{k_x k_y k_0^2 \sin(k_1 h)}{\beta^2 T_e} \right] j_x$$

$$\tilde{E}_z(k_x, k_y, h) = \frac{-j}{\omega \epsilon_0} \frac{k_1 k_x \sin(k_1 h)}{T_m} j_x$$

Comparing expressions with matrix relationship

$$\begin{bmatrix} \bar{E}_x \\ \tilde{E}_y \end{bmatrix} = \begin{bmatrix} \tilde{Z}_{xx} & \tilde{Z}_{xy} \\ \tilde{Z}_{yx} & \tilde{Z}_{yy} \end{bmatrix} \begin{bmatrix} \bar{j}_x \\ \bar{j}_y \end{bmatrix}$$

We can get the expressions of z terms by solving the above matrix. The above procedure can also be used to determine the green's function for an anisotropic substrate for which the value of the dielectric constant differs in the principal directions.

4.6 MOMENT OF METHOD SOLUTION

AS a first step in the moment of method solution of the unknown current density on the patch is expanded in a set of N expansion or basis modes with unknown complex coefficients in that is

$$\bar{j}_s = \hat{x} \sum_{nx=1}^N i_{nx} j_{nx}(x, y) + \hat{y} \sum_{ny=1}^N i_{ny} j_{ny}(x, y)$$

Where $j(nx)$ and $j(ny)$ are called the known expansion functions or modes and $i(nx)$ and $i(ny)$ are the unknown complex coefficients. The Fourier transform of these functions is defined as:

$$F(j_{ni}) = \iint_S j_{ni} e^{-jk_x x} e^{-jk_y y} dx dy$$

The next step in the moment method solution is to take the inner product of the above equation with respect to the test function

$$\iint_s \bar{E}(\bar{j}_e) \cdot \bar{j}_{ms} ds + \iint_s \bar{E}(\bar{j}_s) \cdot \bar{j}_{ms} ds = 0$$

Using Galerkin's procedure, that is, the testing function identical to the expansion function, we arrive at the matrix equation:

$$[Z]_{N \times N} [I]_{N \times 1} = [V]_{N \times 1}, N = N_x + N_y$$

$$Z_{mn}^{ij} = \frac{-1}{4\pi^2} \iint \left(\iint_s j_{mi} e^{jk_x x} e^{jk_y y} ds \right) \tilde{Z}_{ij} F(j_{ni}) dk_x dk_y$$

The voltage is given by

$$V_m^i = \iint F(j_{mn}) Q_{ZI} e^{jk_x x} e^{jk_y y} dk_x dk_y$$

CHAPTER 1

Various steps involved in Spectral domain full wave analysis

- Set up integral equation from the boundary conditions
- Construct the electric field Green's function
- Find the poles and residue associated with the GF's.
- Construct the MOM matrix associated with the integral equation.
- Find the roots of the complex determinant.
- Solve the matrix equation.
- Find surface current, input impedance and loaded Q.
- Calculate Radiation pattern, Polarization, Directivity, Gain and efficiency.

CHAPTER 5

FULLWAVE ANALYSIS USING FINITE DIFFERENCE TIME DOMAIN METHOD (FDTD)

The finite difference time domain technique is used extensively in the analysis and the design of microstrip antenna. The major difference between FDTD and other numerical techniques is that analytical processing and modeling are almost absent in FDTD. Therefore complex antenna can be analyzed with FDTD. This analysis approach can be used to include the effect of finite size of substrate and ground plane which is very important in design of any microstrip antennas. This technique has number of other advantages over other techniques. It is capable of broadband frequency response because analysis is carried out in the time domain. It analyze complex systems and antennas and also able to analyze structure using different type of materials.

Analysis of any problem using FDTD start with dividing the structure in to various regions based on material properties. The unbounded region if any is bounded by terminating it with absorbing medium or termination such that reflection does not occur. Next the problem physical space is discretized in the form of number of cuboids. The time domain is also discretized with integral size Δt , the structure then excited by an electromagnetic pulse. The wave launched by the pulse is the structure is studied for its propagation behavior. The stabilized time domain waveform is numerically processed to determine the time domain and frequency domain characteristic of the structure.

E- plane radiation pattern for two slots at a distance L is

$$F_E(\phi) = \frac{\sin(k_0(\frac{h}{2})\cos\phi)}{k_0(\frac{h}{2})\cos\phi} \cos(k_0b/2\cos\phi)$$

Where b= length of patch

H- plane radiation pattern for two slots at a distance L is

$$F_H(\theta) = \frac{\sin(k_0b\cos\theta)}{k_0b\cos\theta} \sin\theta$$

Directivity of a single slot microstrip antenna is

$$D = \frac{4b^2\pi^2}{I_1\lambda_0^2}$$

where $I_1 = \int_0^\pi \sin^2\left(\frac{k_0b\cos\theta}{2}\right) \tan^2\theta \sin\theta \, d\theta$

Directivity of a microstrip antenna with a pair of slot is

$$D_s = \frac{2D}{1 + g_{12}}$$

Where $g_{12} = \frac{1}{120\pi^2} \int_0^\pi \frac{\sin^2(\pi b \cos\theta) \tan^2\theta \sin\theta j_0\left(\frac{2\pi a}{\lambda} \sin\theta\right)}{G} d\theta$

$J_0(x)$ is the zeroth order Bessel function with argument x

$$G = \frac{1}{R_r}$$

Where R_r is the Radiation Resistance

The relationship between electric field and axial ratio is

$$AR = \sqrt{\frac{1 + \left[\frac{E_x}{E_y} \right]^2 + T}{1 + \left[\frac{E_x}{E_y} \right]^2 - T}}$$

AR is the axial ratio

$$\text{Where } T = \sqrt{1 + \left[\frac{E_x}{E_y} \right]^4 + 2 \left[\frac{E_x}{E_y} \right]^2 \cos(2\psi)}$$

Where ψ = phase of E_x/E_y

efficiency of a microstrip antenna is

$$G = eD$$

Efficiency according to cavity model is given by the equation

$$e = \frac{Q_d Q_c Q_{sw}}{Q_{sw} Q_c Q_D + Q_{sw} Q_c Q_R + Q_R Q_d Q_c + Q_{sw} Q_R Q_D}$$

$$Q_d = \frac{1}{\tan \delta}$$

$$Q_C = \frac{1}{2} \eta_0 \mu_r \left(\frac{k_0 h}{R_s} \right)$$

$$R_s = \sqrt{\frac{\omega \mu_0}{2\sigma}}$$

$$Q_R = \frac{2\omega W_{es}}{P_r}$$

$$W_{es} = \frac{\epsilon_0 \epsilon_r L W V_0^2}{8h}$$

Where W_{es} is the energy stored

Where L = length of patch and W = width of patch

Power radiated in to space

$$P_r = \frac{V_0^2 A \pi^4}{23040} \left[(1-B) \left(1 - \frac{A}{15} + \frac{A^2}{420} \right) + \frac{B^2}{5} \left(2 - \frac{A}{7} + \frac{A^2}{189} \right) \right]$$

$$A = \left(\frac{\pi W}{\lambda_0} \right)^2$$

$$B = \left(\frac{2L}{\lambda_0} \right)^2$$

$$Q_{SW} = Q_r \left(\frac{e_r^{hed}}{1 - e_r^{hed}} \right)$$

$$e_r^{hed} = \frac{P_r^{hed}}{P_r^{hed} + P_{sw}^{hed}}$$

CHAPTER 6

RESULT OBTAINED AFTER WORKING ON COMPUTER SIMULATION TECHNIQUE NAMED AS (CST) MICROWAVE STUDIO

INSTRUCTIONS:

- Frequency Range Is 1 – 20 GHz.
- All Dimensions are in millimeter (mm) and Time in nanoseconds (ns).
- Ground plane is made up of Aluminium having electrical conductivity $3.72 \text{ e } +007$ s/m, $\mu=1.0$ and its length is 10mm, breadth is 6mm and height is 0.1mm.
- Substrate is made up of Roger TMM having $\epsilon = 3.4$, $\mu=1.0$ and its length is 10mm, breadth is 6mm and height is 1.91mm.
- Patch is made up of brass having Electrical conductivity $1.57 \text{ e } +007$ s/m, $\mu=1.0$ and its length is 5mm, breadth is 4mm and height is 0.30mm.
- Microstrip feed line is of copper having Electrical conductivity $5.8 \text{ e } +007$ s/m, $\mu=1.0$ and its length is 3.1mm, breadth is 2.2mm, height is 0.01.

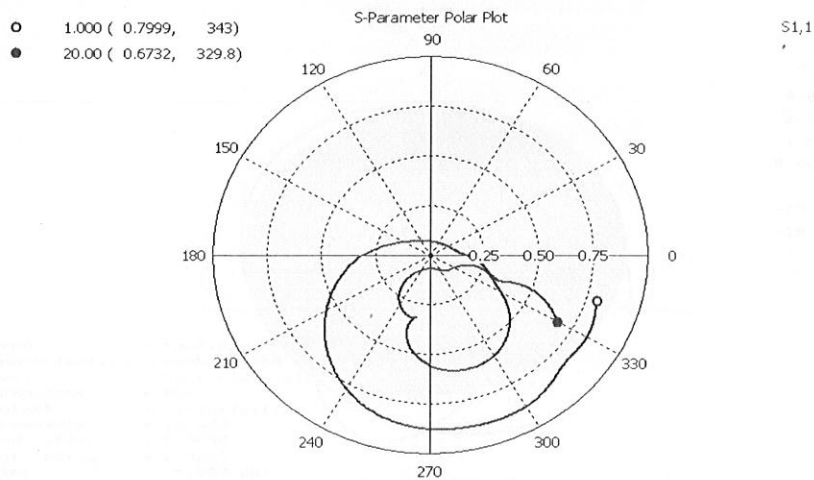


Fig 6.1

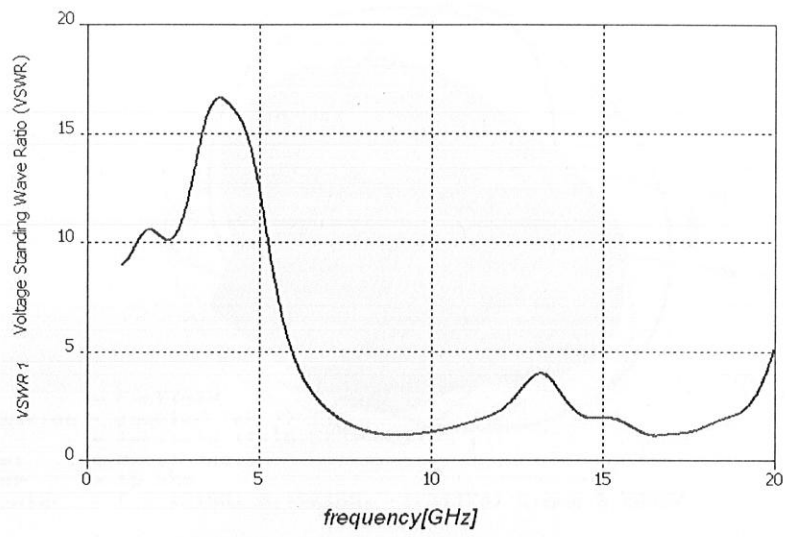


Fig 6.2

Warning: Farfield is inaccurate!

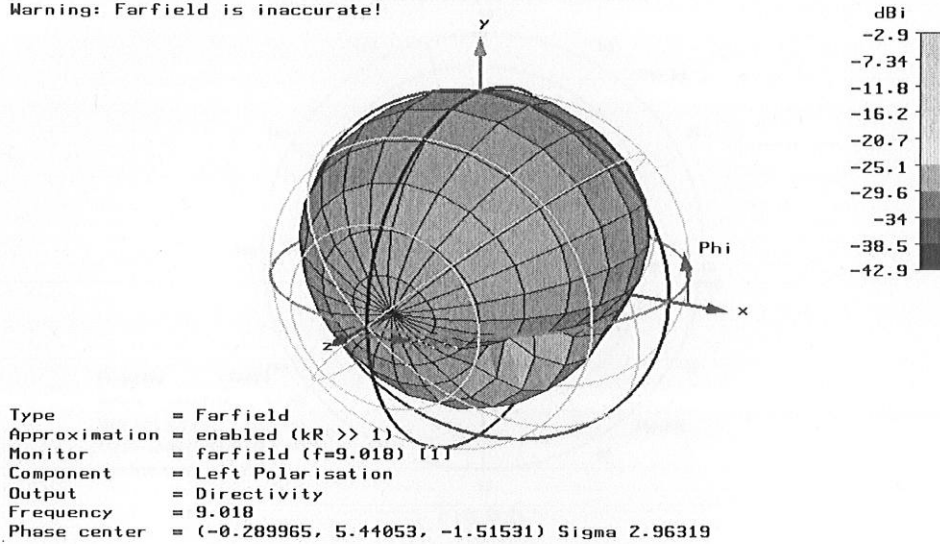


Fig 6.3

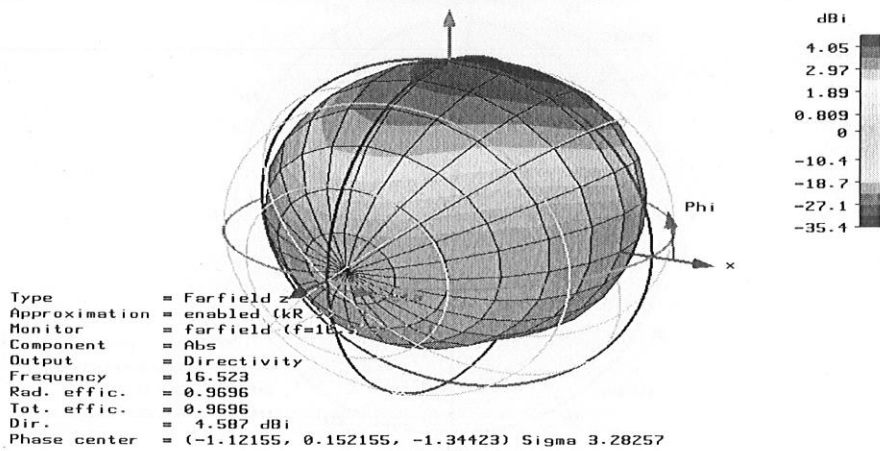
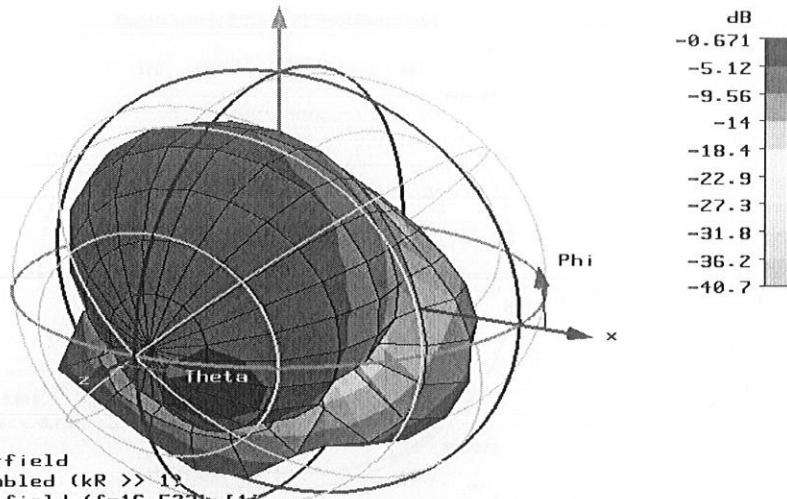


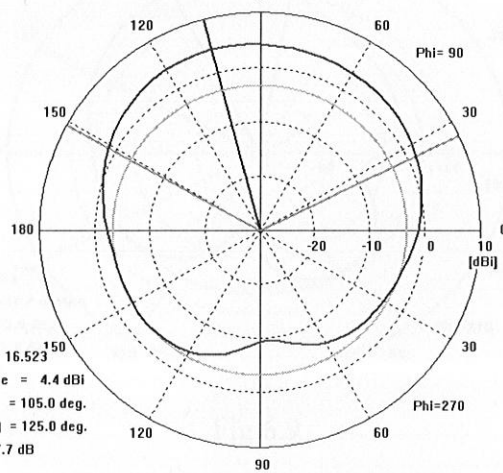
Fig 6.4



Type = Farfield
 Approximation = enabled ($kR \gg 1$)
 Monitor = farfield ($f=16.523$) Hz
 Component = Axial Ratio
 Frequency = 16.523
 Phase center = (-1.12155, 0.152155, -1.34423) Sigma 3.28257

Fig 6.5

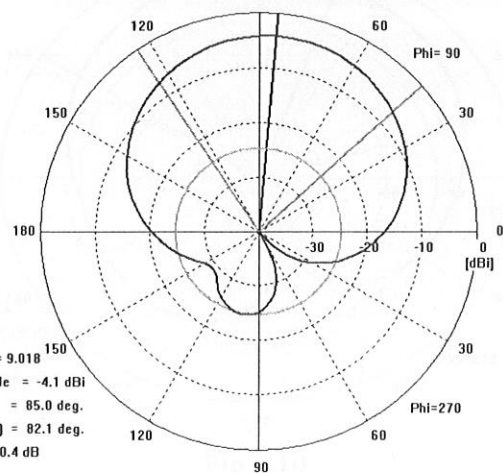
Farfield 'farfield (f=16.523) [1]' Directivity_Abs(Theta)



Frequency = 16.523
 Main lobe magnitude = 4.4 dBi
 Main lobe direction = 105.0 deg.
 Angular width (3 dB) = 125.0 deg.
 Side lobe level = -7.7 dB

Fig 6.6

Farfield 'farfield (f=9.018) [1]' Directivity_Right Polarisation(Theta)



Frequency = 9.018
 Main lobe magnitude = -4.1 dBi
 Main lobe direction = 85.0 deg.
 Angular width (3 dB) = 82.1 deg.
 Side lobe level = -20.4 dB

Fig 6.7

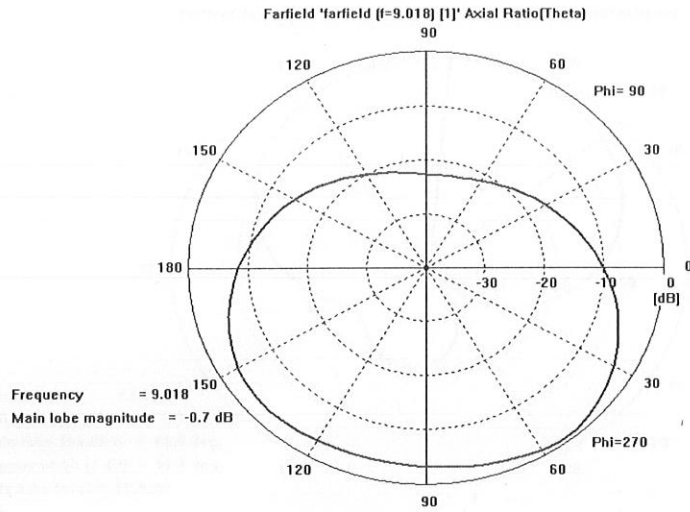


Fig 6.8

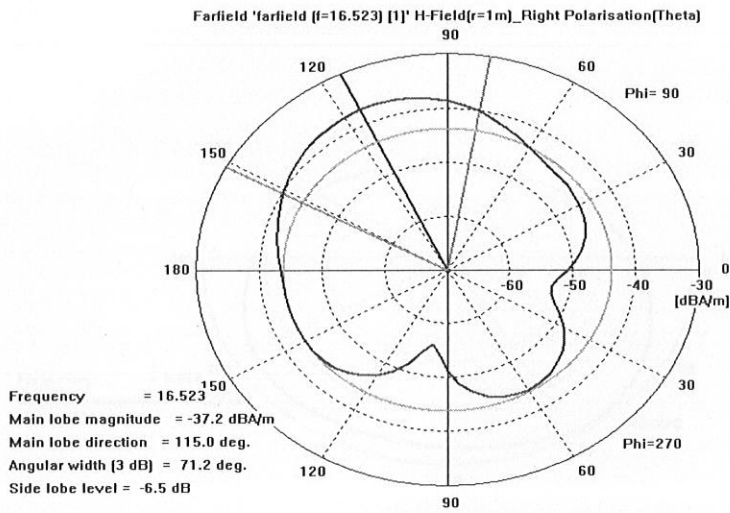


Fig 6.9

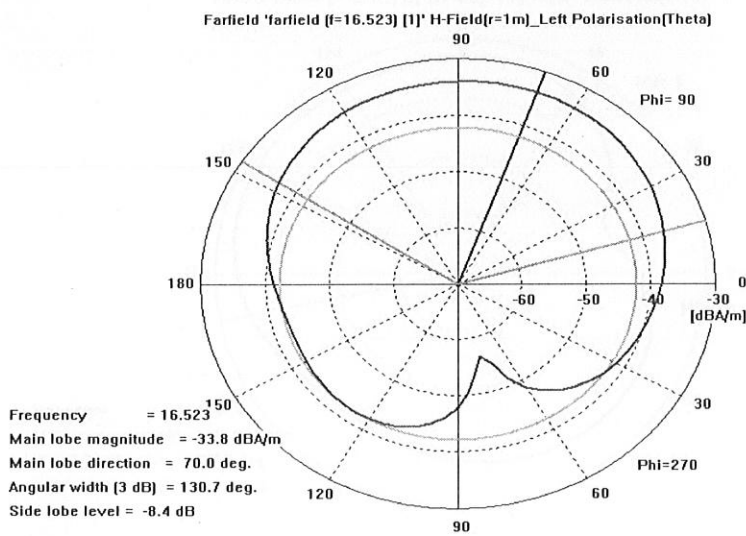


Fig 6.10

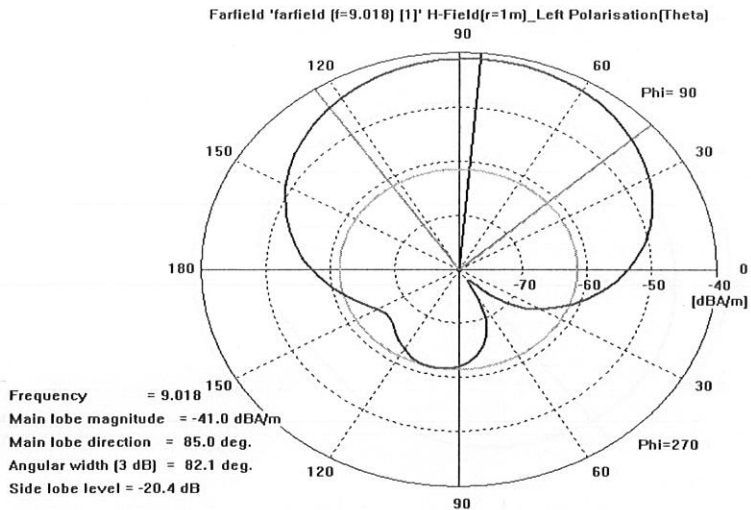


Fig 6.11

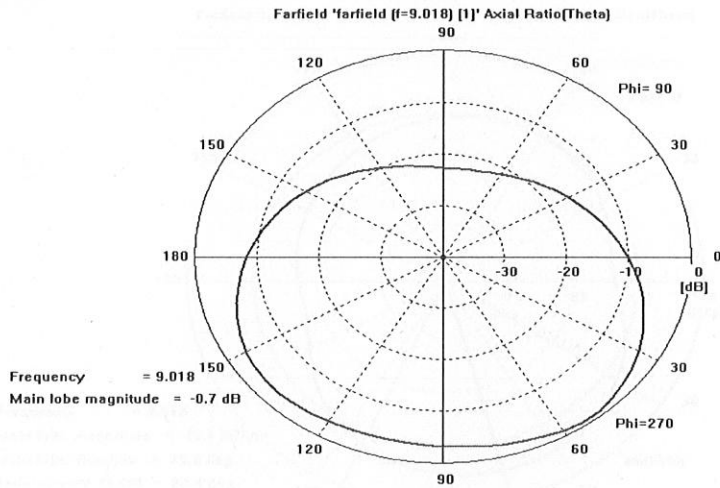


Fig 6.12

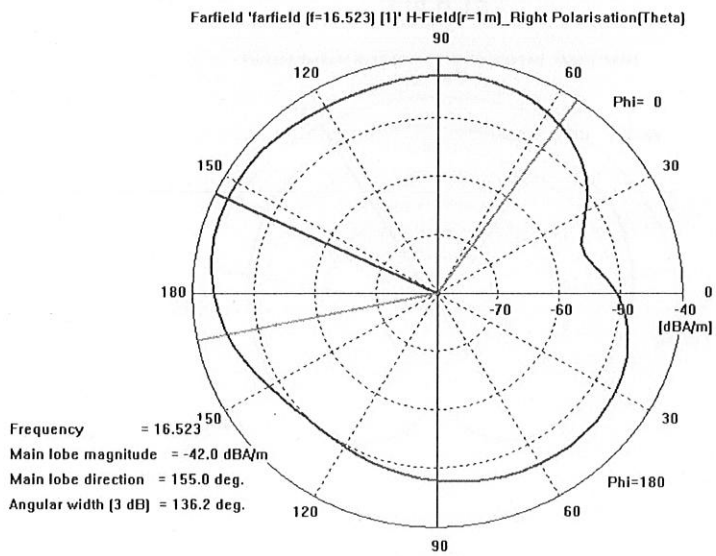


Fig 6.13

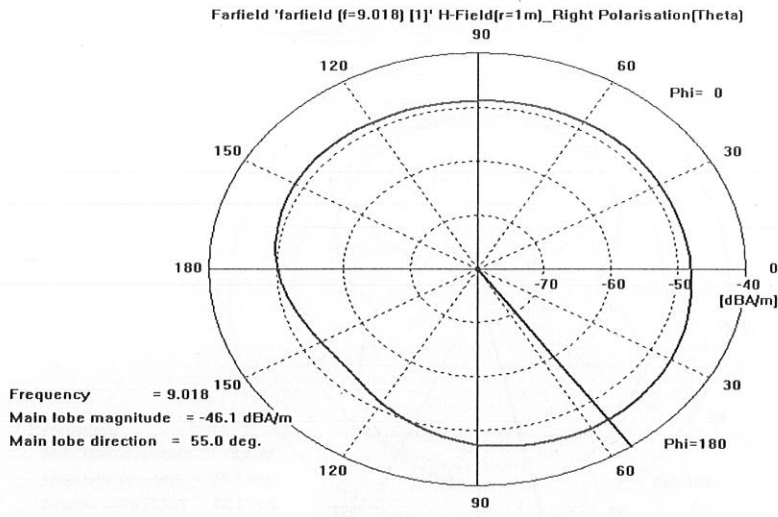


Fig 6.14

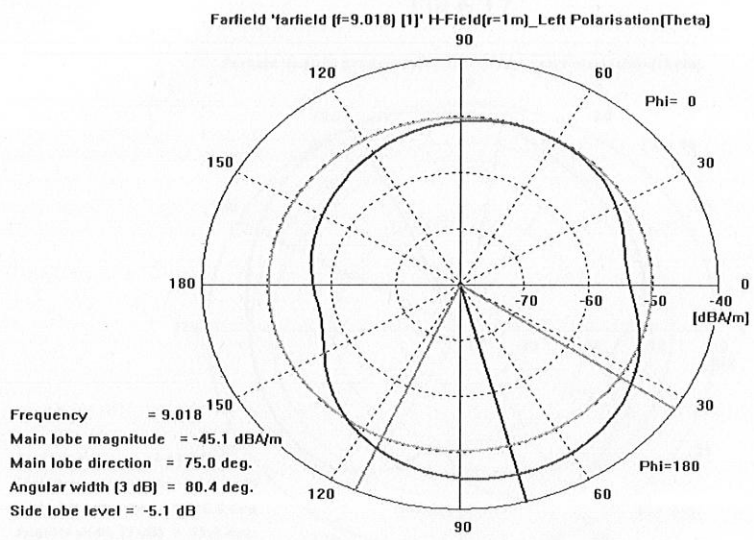


Fig 6.15

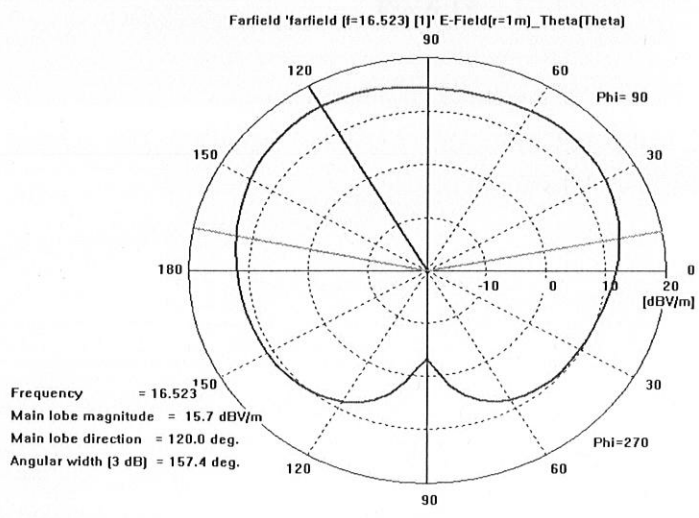


Fig 6.16

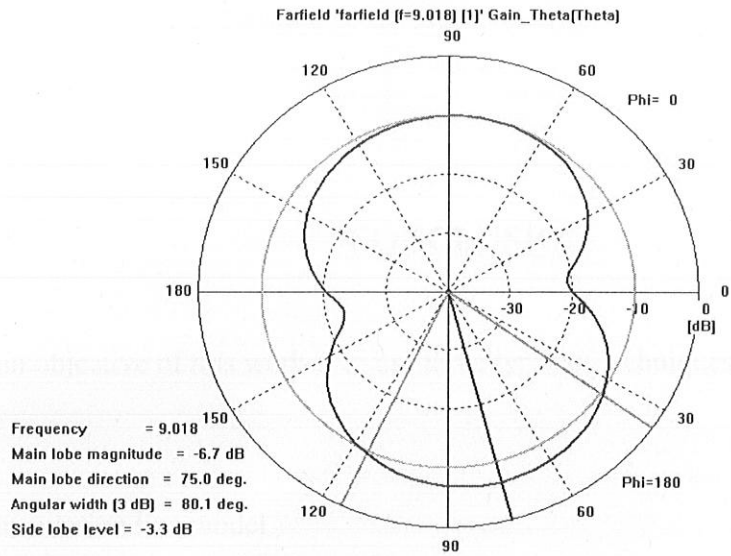


Fig 6.17

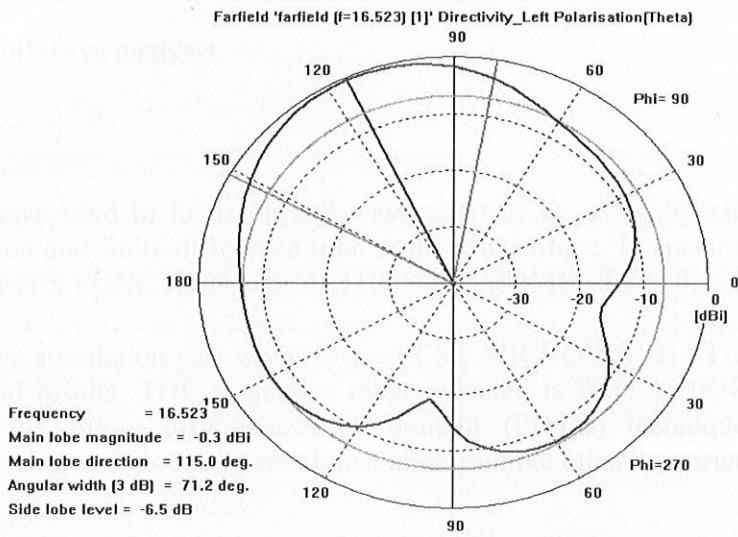


Fig 6.18

REFERENCES

1. J. J. Doherty and P. Bhattacharya, *Microstrip Antennas*, McGraw-Hill, 1992.
2. J. R. James, P. S. Hall, and C. Wood, *Microstrip Antennas: Theory and Design*, London, U.K., Peter Peregrinus, 1981.
3. J. R. James and P. S. Hall, *Microstrip Antennas*, London, U.K., Peter Peregrinus, 1989.

CONCLUSION

The main objective of this work is to use three types of techniques namely:

- 1) Transmission line model
- 2) Cavity model
- 3) Full wave analysis

We have tried to focus on full wave analysis by using Spectral – domain full wave solution and finite-difference-time domain technique. In spectral domain we have used GREEN'S FUNCTION and METHOD OF MOMENTS in the analytical part.

For the simulation part we have used CST MICROWAVE STUDIO Software to attain desired results. THE frequency range selected is from 1-20GHZ. The CST Software uses the Finite difference time domain (FDTD) technique in which analytical processing and modeling are almost absent unlike other numerical techniques.

4. D. M. Pozar, "Microstrip Antenna Aperture Coupled to a Microstrip Line," *IEEE Trans. Antennas Propagat.*, vol. 37, pp. 677-682, June 1989.
5. D. M. Pozar and H. Kaufman, "Increasing the Bandwidth of a Microstrip Antenna by Aperture Coupling," *Electron Lett.*, vol. 23, pp. 368-369, Apr 1987.
6. D. M. Pozar, "Microstrip Antenna Aperture Coupled to a Microstrip Line," *Electron Lett.*, vol. 21, pp. 49-50, Jan 1985.
7. C. H. Chu, "A Theory of the Aperture-Coupled Microstrip Antenna," *IEEE Antennas and Propagation Symp. Dig.*, pp. 23-24, 1988.
8. R. Q. Lee, X. F. Tang, and J. B. Beker, "Characterization of a Two-Layer Microstrip Antenna," *IEEE Antennas and Propagation Symp. Dig.*, pp. 23-24, 1988.
9. C. H. Tsai, Y. M. Hwang, F. K. Seng, and R. Dietrich, "Aperture-Coupled Patch Antennas with Wide Bandwidth and Dual Polarization Capability," *IEEE Antennas and Propagation Symp. Dig.*, pp. 946-949, 1988.
10. A. Hryshchuk, B. Clarke, and M. Cobaci, "Slot-Coupled Stacked Microstrip Antennas," *IEEE Antennas and Propagation Symp. Dig.*, pp. 1108-1111, 1990.

REFERENCES

1. I. J. Bahl and P. Bhartia , Microstrip Antennas Dedham. MA. Artechhouse, 1980
2. J. R. James, P. S.Hall , and C.Wood , Microstrip Antenna Theory and Design.London , U.K. , Peter Peregrinus . 1981
3. J. R . James and P. S. Hall, Handbook of Microstrip Antennas . London , U.K.: , Peter Peregrinus , 1989
4. D. M. Pozar, "Finite Phased Arrays of Rectangular Microstrip Antennas" IEEE Trans. Antennas Propagate, vol. AP-31,pp.740_747,1983.
5. D. H. Schaubert, D. M. Pozar and A. Adrian m," Effect of Microstrip Antenna Substrate Thickness and Permittivity: Comparison of Theories and Experiments IEEE Trans. Antennas Propagate, vol. 37, pp.677-682,June 1989.
6. D. M. Pozar and B. Kaufman , "Increasing the Bandwidth of a Microstrip Antenna by Proximity Coupling ." Electron.Lett,vol.23,pp.368-369,Apr.1987.
7. D. M .Pozar , "Microstrip Antenna Aperture Coupled to a Microstrip Line "Electron.Lett,vol.21.pp.49-50,Jan.1985.
8. H. K. Smith and P .E. Mayes , " Mode Purity of Rectangular Parch Antennas With Post and Aperture Excitation" in Allerton Antenna Symp.Dig.,pp.363-375,1989.
9. D. M. Pozar and R. W. Jackson , " An Aperture Coupled Microstrip Antenna with a Proximity Feed on a Perpendicular Substrate "IEEE Trans.Antennas Propagate.,vol.AP-35,pp.728-731,June 1987.
10. A. Sabban , " A new Broadband Staggered Two Layer Microstrip Antenna "in IEEE Antennas and Propagation Symp.Dig,pp.63-66,1983.
11. C. H. Chen , A. Tulintseff and M. Sorbello ," Broadband two layer Microstrip Antenna "in IEEE Antennas and Propagation Symp.Dig,pp.251-254,1984.
12. R. Q. Lee, K. F. Lee and J. Bobinchak ,"Characteristics of a Two Layer Electromagnetically Coupled Rectangular Patch Antenna "Electron.Lett.vol.23,pp.1070-1072,Sept.1987.
13. C. H. Tsao , Y. M. Hweng , F. Kilburg , and F. Dietrich" Aperture coupled Patch Antennas with wide bandwidth and dual polarization capabilities "in IEEE Antennas and Propagation Symp.Dig,pp.936-939,1988
14. A. Ittipiboon , B. Clarke and M. Cuhaci ," slotcoupled stacked Microstrip Antenna "in IEEE Antennas and Propagation Symp.Dig,pp.1108-1111,1990.

15. J. T. Aberle and D. M. Pozar ,” Rigorous and Versatile Solutions for Probe Feed Microstrip Patched Antennas and Arrays “in IEEE Antennas and Propagation Symp.Dig,pp.350-353,1990.
16. D. M. Pozar and S. M. Voda,” Rigorous Analysis of a microstrip line fed patch antenna”IEEE Trans.Antennas Propagate,vol.AP-35,pp.1343-1350,Dec.1987.
17. L. Barlatey , J. R. Mosig and T. Sphicopoulos ,” Analysis of stacked microstrip patches with a mixed potential integral equations “IEEE Trans.Antennas Propagate,vol.38,pp.608-615 May 1990.
18. P. L. Sullivan and D. H. Schaubert ,” Analysis of an Aperture coupled microstrip antenna “IEEE Trans.Antennas Propagate,vol.AP-34,pp-977-984,Aug.1986.
19. D. M .Pozar ,” A reciprocity method of analysis for printed slot and slot coupled microstrip antennas” IEEE Trans.Antennas Propagate,vol.AP-34,pp-1439-1446,Dec 1986.
20. F. K. Schwing ,” Millimeter wave antennas “Proceedings IEEE,80(1),92-102(1992).
21. Z. Fan, J. Huang ,” Hankel transform domain analysis of an angular ring microstrip antenna with year gap “Int.Conf.Computation Electromag.312-314(1991).
22. R. Garg , P. Bhartia , I. Bahl ,A. Ittipiboon, “Microstrip antenna design handbook”(Artech House,Inc.Boston.USA 2001).
23. A. A. Kishk and L. Shafi,” The effect of various parameters of circular micro strip antenna on their radiation efficiency and the mode of excitation. IEEE Trans.Antennas Propagate,vol.AP-34,pp.969-977,1986.
24. C. C. Liu,A. Hessel and J. Shmoys,” Performance of probe fed rectangular microstrip patch element phased arrays ,” . IEEE Trans.Antennas Propagate,vol.36,pp.1501-1509,Nov.1988.
25. C. Wu,J. Wang,R. Fralich and J. Litva,”Study on a series fed aperture coupled microstrip patch array,” IEEE Trans.Antennas Propagate,vol.36,pp.1762-1765,1990.
26. P. S. Hall and C. M. Hall ,”Coplaner corporate feed effects in microstrip patch array design,”Proc.Inst.Elect.Eng.pt.h.vol.135,pp.180-186,June 1988.

27. M. Himdi, J. P. Daniel and C. Terret, "Analysis of aperture coupled microstrip antenna using cavity method," *Electron Lett*, vol.25pp.391-392, Mar.1989.
28. R. J. Maillous, J. F. Melivenna and N. P. Kernweis, "Microstrip array technology," *IEEE Trans. Antennas Propagate*, vol.AP-29, pp.25-37, Jan.1981.
29. W. F. Richard, Y. T. Lo and D. Harrison, "An improved theory for microstrip antennas and applications," *IEEE Trans. Antennas Propagate*, vol.AP-29, pp.38-46, Jan.1981.
30. P. B. Katehi and N. G. Alexopoulos, "On the modeling of electromagnetically coupled microstrip antennas," *IEEE Trans. Antennas Propagate*, vol.AP-32, pp.1179-1186, Nov.1984.
31. T. Itoh, *Numerical Techniques of microstrip and millimeter wave passive structures.* (John Wiley & Sons, New York 1989).
32. K. R. Carver and J. W. Mink, "Microstrip Antenna Technology," *IEEE Trans. Antennas Propagate.*, volume.AP-29, pp.2-24. Jan.1981.